# Background-Free Microwave Signal Generation Based on Unbalanced Temporal Pulse Shaping

Wen Ting Wang, Ming Li, Shu Qian Sun, Chao Wang, Ye Deng, and Ning Hua Zhu

***Abstract*— We propose a new method to generate background-free high-frequency pulsed microwave signal based on an unbalanced temporal optical pulse shaping (TPS) system and balanced photodetection. The proposed system consists of a polarization modulator and an unbalanced TPS system realized by two conjugate dispersion elements. The carrier frequency of the pulsed microwave signal could be tuned by changing the residual dispersion of the TPS. The proposed method is theoretically analyzed and experimentally demonstrated. The experimental results show that the carrier frequency of the generated microwave pulse could be tuned over a broad frequency range. Moreover, the generated microwave pulse signal is background-free by suppressing the baseband frequency components using balanced photodetection.**

***Index Terms*— Pulsed microwave signal, unbalanced temporal pulse shaping, balanced photo-detection.**

## I. Introduction

PHOTONIC generation of pulsed microwave signals has attracted considerable attention for its widespread applications in radar systems, microwave tomography, broadband wireless access networks, and warfare systems [1]–[3]. Compared with its electrical counterparts, photonic generation of microwave signals has some advantages such as wide bandwidth, low loss transmission, and low power consumption, and immunity to electromagnetic interference (EMI) [4]. Up to now, various configurations have been reported to generate microwave pulses using photonic techniques. High frequency microwave pulses are generated by simply multiplying the low frequency microwave and then truncating the continuous wave into pulses in the time domain [5]. It can be also generated using optical spectral-shaping incorporating with frequency-to-time mapping [6], which is a powerful and promising method. The key component in these systems is an optical spectral shaper, which is usually realized using a fiber comb filter or a spatial light modulator (SLM) [7]. One of the advantages of SLM is that its transmission response is flexibly reconfigurable in real time so that an arbitrary optical waveform could be easily generated. However, the SLM-based microwave pulse generation system is bulky and complicated since it involves space-to-fiber and fiber-to-space coupling. As an alternative candidate for spectral shapers, a fiber comb filter with higher stability and lower power consumption is smaller [8]. However, the spectral response keeps unchanged once it is fabricated. C. Wang proposed and experimentally demonstrated a powerful method to generate a frequency-multiplied microwave pulse using a unbalanced TPS, which consists of two dispersive elements with opposite dispersion but non-identical in magnitude and an electro-optic modulator located between the two dispersive elements [9]. One of the limitations in this system is that the generated microwave pulse has baseband frequency components in the electrical spectrum which would interfere with other narrow-band serves. J.D. Mckinney proposed a powerful method to eliminate the baseband components using polarization pulse shaping. However, the proposed system is bulky [10].

In this letter, we propose a new method to generate background-free pulsed microwave signals based on unbalanced TPS and balanced photo-detection. A length of dispersion compensating fiber (DCF) and single mode fiber (SMF) are used as two dispersive elements in this system. A joint use of a PolM, a Polarization controller (PC) and a polarization beam splitter (PBS) is equivalent to two intensity modulators with differential response. The frequency of the pulsed microwave signal could be tuned by changing the residual dispersion of the TPS. The experimental results show that the frequency of the generated microwave pulse could be tuned. Moreover, the generated microwave pulse signal is background-free by suppressing the baseband frequency components using balanced photo-detection.

## II. Principal

The schematic diagram of the proposed background-free pulsed microwave signal generation system based on unbalanced TPS and balanced photo-detection is shown in Fig. 1(a). The proposed system mainly includes a mode-locked laser (MLL), DCF and SMF regarding as two dispersive elements, two polarization controllers (PCs), a PolM and a polarization beam splitter (PBS). A transform-limited Gaussian pulse, $g(t) = \exp(-t^2/2\tau_0^2)$, is emitted from MLL, where $\tau_0$ is the standard deviation. We firstly assume that the values of the third-order dispersion (TOD) of the system

Manuscript received November 10, 2015; revised January 3, 2016; accepted January 4, 2016. Date of publication January 12, 2016; date of current version March 10, 2016. This work was supported by the National Natural Science Foundation of China under Grant 61377069, Grant 61335005, Grant 61321063, and Grant 61090391.

W. T. Wang is with the State Key Laboratory on Integrated Optoelectronics, Institute of Semiconductors, Chinese Academy of Sciences, Beijing 100083, China, and also with the Center for Free-Electron Laser Science, Deutsches Elektronen-Synchrotron, Hamburg 22607, Germany (e-mail: wtwang13@semi.ac.cn).

M. Li, S. Q. Sun, Y. Deng, and N. H. Zhu are with the State Key Laboratory on Integrated Optoelectronics, Institute of Semiconductors, Chinese Academy of Sciences, Beijing 100083, China (e-mail: ml@semi.ac.cn; sqsun@semi.ac.cn; ydeng@semi.ac.cn; nhzhu@semi.ac.cn).

C. Wang is with the School of Engineering and Digital Arts, University of Kent, Canterbury CT27NT, U.K. (e-mail: c.wang@kent.ac.uk).

Color versions of one or more of the figures in this letter are available online at http://ieeexplore.ieee.org.

Digital Object Identifier 10.1109/LPT.2016.2517181

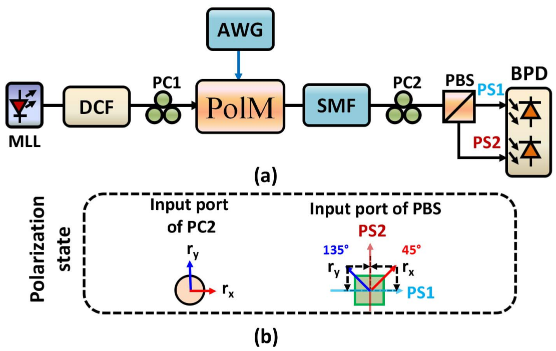


Fig. 1. (a) The schematic diagram of the proposed system for background-free pulsed microwave signal. MLL: mode-locked laser; DCF: dispersion compensating fiber; PC1, PC2: polarization controllers; AWG: arbitrary waveform generator; PolM: polarization modulator; SMF: single mode fiber; PBS: polarization beam splitter; BPD: balanced photo-detector; (b) the polarization direction of signals at the input port of PC2 and PBS.

are small and only the group delay dispersion (GVD) is considered. The normalized transfer function of the SMF and DCF could be represented as $H_1(\omega) = \exp(-i\ddot{\Phi}_1\omega^2/2)$ and $H_2(\omega) = \exp(-i\ddot{\Phi}_2\omega^2/2)$, where $\ddot{\Phi}_1$, $\ddot{\Phi}_2$ ($ps^2/rad$) are their GVD, respectively. The proposed unbalanced TPS system can be considered as a typical TPS system with a pair of complementary dispersion elements, followed by a residual dispersion element with a transfer function of $H_\Delta(\omega) = \exp(-i\Delta\ddot{\Phi}\omega^2/2)$, where $\Delta\ddot{\Phi} = \ddot{\Phi}_1 + \ddot{\Phi}_1$. In our proposed system, the modulation signal applied to the PolM is a sinusoidal signal. Under the small signal modulation condition, the modulation function of the PolM can be written as [11]

$$E_{PolM} = \begin{bmatrix} E_x \\ E_y \end{bmatrix} = \begin{bmatrix} \exp\left(i\beta\cos(2\pi f_m t)\right) \\ \exp\left(-i\beta\cos\left(2\pi f_m t\right) - j\theta\right) \end{bmatrix} \tag{1}$$

where $\beta$ is the phase modulation index, $f_m$ is the frequency of the microwave drive signal applied to the PolM and $\theta$ is phase difference between $E_x$ and $E_y$ which can be tuned by changing the DC bias of the PolM. When the phase difference $\theta = \pi/2$, the Jacobi-Anger expansion of Eq. (1) can be expressed as

$$E_{PolM} = \begin{bmatrix} E_x \\ E_y \end{bmatrix} = \begin{bmatrix} J_0(\beta) + 2iJ_1(\beta)\cos(2\pi f_m t) \\ -iJ_0(\beta) - 2J_1(\beta)\cos(2\pi f_m t) \end{bmatrix} \tag{2}$$

where $J_n(\beta)$ is the n-order Bessel function of the first kind. If the DCF has an adequate dispersion, i.e., $\ddot{\Phi}_1 \gg \tau_0^2$, the output signal of the typical TPS system is given by [10]

$$\begin{aligned} s(t) &= \frac{1}{|\ddot{\Phi}_1|} g(t) * E_{PolM}(\omega)\big|_{\omega_{RF}=t/\ddot{\Phi}_1} = \begin{bmatrix} s_x(t) \\ s_y(t) \end{bmatrix} \\ &= \frac{\sqrt{2}}{2}\begin{bmatrix} J_0(\beta)g(t) + iJ_1(\beta)\left[g(t-T_1) + g(t+T_1)\right] \\ iJ_0(\beta)g(t) - J_1(\beta)\left[g(t-T_1) + g(t+T_1)\right] \end{bmatrix} \end{aligned} \tag{3}$$

where $E_{PolM}$ $(\omega)$ is the Fourier transform of $E_{PolM}(t)$, $*$ denotes the convolution operation, and $T_1 = \omega_m\ddot{\Phi}_1$.

The signal at the output point of the entire unbalanced TPS system $r(t)$ can be obtained by propagating $s(t)$ through the residually dispersive element. If the residually dispersive element has an adequate dispersion, $\Delta\ddot{\Phi} \geq T_1^2/4\pi$, then $r(t)$ can be approximated by the Fourier transform of $s(t)$

$$\begin{aligned} r(t) &= \exp\left(\frac{it^2}{2\Delta\ddot{\Phi}}\right) S(\omega)\big|_{\omega=t/\Delta\ddot{\Phi}} = \begin{bmatrix} r_x(t) \\ r_y(t) \end{bmatrix} \\ &= \frac{\sqrt{2}}{2}\exp\left(\frac{it^2}{2\Delta\ddot{\Phi}}\right) G\left(\frac{t}{\Delta\ddot{\Phi}}\right) \\ &\quad \times \begin{bmatrix} J_0(\beta) + 2iJ_1(\beta)\cos\left(\frac{T_1 t}{\Delta\ddot{\Phi}}\right) \\ -iJ_0(\beta) - 2J_1(\beta)\cos\left(\frac{T_1 t}{\Delta\ddot{\Phi}}\right) \end{bmatrix} \end{aligned} \tag{4}$$

As can be seen in Fig. 1(b), by tuning the polarization controller attached before PBS (PC2), $r_x(t)$ is oriented at 45 degree and $r_y$ (t) is oriented at 135 degree to the X-axis, respectively. After propagating through PBS, the electrical field of signal will be given by:

$$r'(t) = \begin{bmatrix} r'_x(t) \\ r'_y(t) \end{bmatrix} = \frac{\sqrt{2}}{2}\begin{bmatrix} r_x(t) - r_y(t) \\ r_x(t) + r_y(t) \end{bmatrix} \tag{5}$$

where

$$\begin{aligned} r'_x(t) &= \frac{1}{2}\exp\left(\frac{it^2}{2\Delta\ddot{\Phi}}\right) G\left(\frac{t}{\Delta\ddot{\Phi}}\right) \\ &\quad \times \left\{ \begin{array}{l} J_0(\beta) + 2J_1(\beta)\cos\left(\frac{T_1 t}{\Delta\ddot{\Phi}}\right) \\ +i\left[J_0(\beta) + 2J_1(\beta)\cos\left(\frac{T_1 t}{\Delta\ddot{\Phi}}\right)\right] \end{array} \right\} \end{aligned} \tag{6}$$

$$\begin{aligned} r'_y(t) &= \frac{1}{2}\exp\left(\frac{it^2}{2\Delta\ddot{\Phi}}\right) G\left(\frac{t}{\Delta\ddot{\Phi}}\right) \\ &\quad \times \left\{ \begin{array}{l} J_0(\beta) - 2J_1(\beta)\cos\left(\frac{T_1 t}{\Delta\ddot{\Phi}}\right) \\ -i\left[J_0(\beta) - 2J_1(\beta)\cos\left(\frac{T_1 t}{\Delta\ddot{\Phi}}\right)\right] \end{array} \right\} \end{aligned} \tag{7}$$

Then the optical signal is detected in the two PDs, resulting in photocurrents as follows:

$$I_1 = \frac{1}{2}G^2\left(\frac{t}{\Delta\ddot{\Phi}}\right)\left[J_0(\beta) + 2J_1(\beta)\cos\left(\frac{T_1 t}{\Delta\ddot{\Phi}}\right)\right]^2 \tag{8}$$

$$I_2 = \frac{1}{2}G^2\left(\frac{t}{\Delta\ddot{\Phi}}\right)\left[J_0(\beta) - 2J_1(\beta)\cos\left(\frac{T_1 t}{\Delta\ddot{\Phi}}\right)\right]^2 \tag{9}$$

When the two output signals are injected into the PBS, the photocurrent can be expressed as:

$$\begin{aligned} I_{BPD} &= I_1 - I_2 = 4J_0(\beta)J_1(\beta)G^2\left(\frac{t}{\Delta\ddot{\Phi}}\right)\cos\left(\frac{T_1 t}{\Delta\ddot{\Phi}}\right) \\ &= K\exp\left(-\frac{t^2}{2\tau_0^2}\right)\cos\left(\frac{T_1 t}{\Delta\ddot{\Phi}}\right) \end{aligned} \tag{10}$$

where $K = 4J_0(\beta)J_1(\beta)$ is the time-independent constant and $\tau = \Delta\ddot{\Phi}/\tau_0$ is full width at half maximum of the output pulse. Thus, a background-free microwave signal with a Guassian envelop is generated. The new carrier frequency is

$$\omega_{RF} = \left|\frac{T_1}{\Delta\ddot{\Phi}}\right| = \omega_m\left|\frac{\ddot{\Phi}_1}{\Delta\ddot{\Phi}}\right| \tag{11}$$

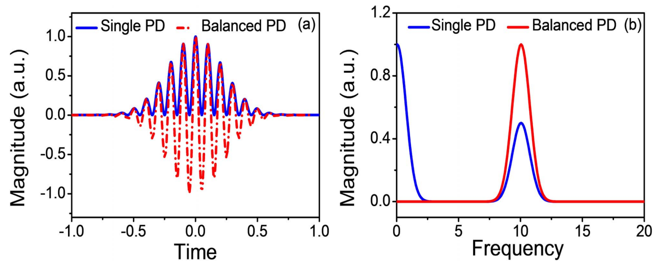


Fig. 2. Simulated results for the microwave pulse generation, (a) the simulated electrical waveform, (b) the simulated electrical spectrum.

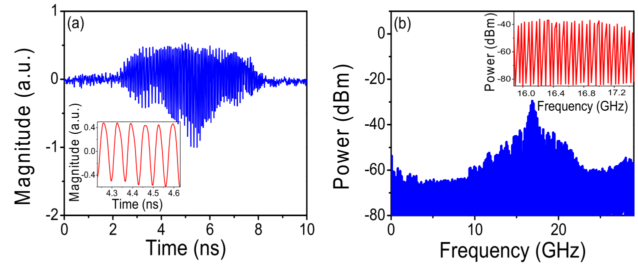


Fig. 3. (a) Measured electrical waveform of the generated microwave pulse, (b) and its electrical spectrum. Inset figures are their zoom-in views.

From Eq. (11), we can conclude that the output carrier frequency is determined by both dispersions of two dispersive elements and the frequency of microwave driven signal. It is worth noting that the frequency multiplication factor $M = \ddot{\Phi}_1/\Delta\ddot{\Phi}$ cannot be infinite. As mentioned before, the residual dispersion has to satisfy the condition $\Delta\ddot{\Phi} \geq T_1^2/4\pi$ to achieve a Fourier transform of the signal. Thus the upper limit of the frequency multiplication factor can be written as $M \leq 4\pi/\omega_m^2\ddot{\Phi}_1$. The key significance of the proposed approach is that the output microwave signal is background-free thanks to the use of PolM and BPD. In addition, the carrier frequency can be tuned by changing the length of DCF or SMF.

Fig. 2 shows the simulated results. Fig. 2 (a) shows the waveform of the generated microwave pulse. The waveform in the red dashed line is generated based on balanced photo-detection and that in the blue solid line is generated based on single-ended detection. The corresponding Fourier transform spectra are shown in Fig. 2 (b). We could obtain the high frequency microwave pulse for both the single-ended detection and the balanced detection. However, it is obviously observed that strong low-frequency components appear in the single-ended detection case and the amplitude of the generated microwave pulse is half of that achieved by the balanced detection. Therefore, the balanced photo-detection has higher power efficiency and no strong low frequency components. The generated microwave signal is background free and its power is enhanced. It is worth noting that only the GVD is considered in our proposed system. This is reasonable for fibers with a length less than 70 km [10]. For a larger dispersive element, the TOD has to be considered and a chirped microwave pulse would be generated.

## III. Experiment

We carried out the experiment based on the setup shown in Fig. 1 to verify the proposed scheme. An MLL (Pritel, 1807-13-048) is used to emit an ultra-short optical pulse train with an average output power of 29.7 mW and a full width at half maximum of 120 fs and a pulse repetition rate of 50.8 MHz. The PolM (Versawave, 0236R03) has a 3-dB bandwidth of 40 GHz and a half-wave voltage of 3.5 V. A sinusoidal microwave signal emitting from an AWG (Tektronix AWG70001A) with an output power of −10 dBm is injected into the PolM such that small signal modulation condition is satisfied. The frequency of the driven

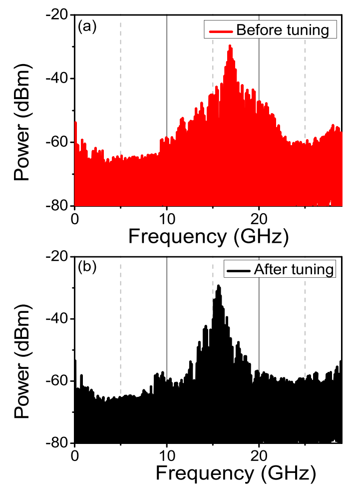


Fig. 4. Measured electrical spectra (a) before tuning, (b) after tuning.

microwave signal was 5 GHz. The DCF (G.655C/250) and SMF (G6520D) are used as the first and the second dispersive elements, respectively. The dispersion of DCF is not matched to that of the SMF so that the unbalanced TPS system is achieved.

The BPD ($u^2$t, BPRV2125AM) has a bandwidth of 40 GHz and a conversion gain of 110 V/W. The generated microwave pulse signal is recorded by a high-speed oscilloscope. Its electrical spectrum is measured by an electrical spectrum analyzer (ESA). Fig. 3 (a) shows the generated waveform obtained by the BPD, which is actually the amplitude summation of the two generated waveforms in the two PDs of the BPD. This waveform was recorded by an oscilloscope (Tektronix, DPO73304D). It is obviously observed by Fig 3 (a), the waveform has both positive and negative parts and not a pedestal. The waveform has asymmetrical positive and negative parts which are mainly attributed to the unequal input optical power for the BPD induced by the PBS or the different responsivity of the two PDs in the BPD. From Eq. (8) (9) and (10) we can see that, if the input optical power for the BPD or the response of the two PDs are different, the baseband component cannot be suppressed completely. The duration of generated microwave pulse is about 2.2 ns. The temporal oscillation period of the generated microwave pulse is about 59 ps, which is corresponding to a carrier frequency of 16.949 GHz. Fig.3 (b) shows the measured electrical spectrum of the generated microwave pulse.

The central frequency is 16.9 GHz. The inset of Fig. 3(b) shows the magnifying spectrum at the different frequency span and resolution. The GVD of the DCF is about $(1/2\pi)$ 3190 $ps^2$/rad. The SMF has a dispersion of 17 ps/km. The GVD of the SMF is about - $(1/2\pi)$ 2247 $ps^2$/rad corresponding its length of 16.5 km. As can be seen from Fig. 3 (b), the baseband frequency components are nearly eliminated by the balanced photo-detection. Therefore, the background-free pulsed microwave signal is successfully obtained by the proposed method.

In order to demonstrate the frequency tunability of the generated microwave pulses, the residual dispersion of the system was tuned by changing the length of the SMF. The length of SMF was changed to 15.8 km. Fig. 4 shows the electrical spectra of the generated microwave signal. As can be seen from Fig. 4, the central frequency of the generated microwave signal has been tuned to 15.5 GHz in black line. It is successfully demonstrated that by properly changing the residual dispersion value of the TPS the frequency of the generated microwave pulse signal could be tuned.

## IV. Conclusion

We have proposed and experimentally demonstrated a new method to generate background-free pulsed microwave signals with tunable central frequency based on unbalanced TPS and balanced photo-detection. Since the two dispersive components are not matched in GVD, the entire system is equivalent to a balanced TPS followed by a residual dispersive processor for a second real-time Fourier transform. The central frequency of the generated pulsed microwave signal is tuned by changing the residual dispersive value of the unbalanced TPS. The experimental results show that the generated microwave pulse has a temporal oscillation period of 59 ps and the corresponding central frequency of that is 16.9 GHz. It is worth noting that the electrical spectrum of the generated microwave pulse does not contain baseband frequency components. Moreover, the central frequency of the generated microwave signal could be tuned by changing the length of DCF or SMF.

## References


[1] J. Azaña, N. K. Berger, B. Levit, and B. Fischer, "Reconfigurable generation of high-repetition-rate optical pulse sequences based on time-domain phase-only filtering," *Opt. Lett.*, vol. 30, no. 23, pp. 3228–3231, Dec. 2005.

[2] M. A. Muriel, J. Azaña, and A. Carballar, "Real-time Fourier transformer based on fiber gratings," *Opt. Lett.*, vol. 24, no. 1, pp. 1–3, Jan. 1999.

[3] P. C. Chou, H. A. Haus, and J. F. Brennan, III, "Reconfigurable time-domain spectral shaping of an optical pulse stretched by a fiber Bragg grating," *Opt. Lett.*, vol. 25, no. 8, pp. 524–526, Apr. 2000.

[4] R. E. Saperstein, D. Panasenko, and Y. Fainman, "Demonstration of a microwave spectrum analyzer based on time-domain optical processing in fiber," *Opt. Lett.*, vol. 29, no. 5, pp. 501–503, Mar. 2004.

[5] F. Zhang, X. Ge, S. Pan, and J. Yao, "Photonic generation of pulsed microwave signals with tunable frequency and phase based on spectral-shaping and frequency-to-time mapping," *Opt. Lett.*, vol. 38, no. 20, pp. 4256–4259, Oct. 2013.

[6] H. Chi and J. Yao, "All-fiber chirped microwave pulses generation based on spectral shaping and wavelength-to-time conversion," *IEEE Trans. Microw. Theory Techn.*, vol. 55, no. 9, pp. 1958–1963, Sep. 2009.

[7] J. Chou, Y. Han, and B. Jalali, "Adaptive RF-photonic arbitrary waveform generator," *IEEE Photon. Technol. Lett.*, vol. 15, no. 4, pp. 581–583, Apr. 2003.

[8] Y. Park and J. Azaña, "Optical signal processors based on a time-spectrum convolution," *Opt. Lett.*, vol. 35, no. 6, pp. 796–798, Mar. 2010.

[9] C. Wang, M. Li, and J. Yao, "Continuously tunable photonic microwave frequency multiplication by use of an unbalanced temporal pulse shaping system," *IEEE Photon. Technol. Lett.*, vol. 22, no. 17, pp. 1285–1288, Sep. 1, 2010.

[10] J. D. McKinney, "Background-free arbitrary waveform generation via polarization pulse shaping," *IEEE Photon. Technol. Lett.*, vol. 22, no. 16, pp. 1193–1195, Aug. 15, 2010.

[11] S. Pan and Y. Zhang, "Tunable and wideband microwave photonic phase shifter based on a single-sideband polarization modulator and a polarizer," *Opt. Lett.*, vol. 37, no. 21, pp. 4483–4485, Nov. 2012.